

Dynamic Model of Back-to-Back Converter for System-Level Phasor Simulation

Hisham Mahmood, Samrat Acharya, Francis Tuffner, Priya Mana, Alok Kumar Bharati
Pacific Northwest National Laboratory (PNNL), Richland, WA, USA
 (hisham.mahmood, samrat.acharya, francis.tuffner, priya.mana, ak.bharati)@pnnl.gov

Abstract—The power system is expected to evolve rapidly with the increasing deployment of power electronic interface and conditioning systems, microgrids, and hybrid AC/DC grids. Among power electronic systems, back-to-back (BTB) converters can be a powerful interface to integrate microgrids and networked microgrids. To study the integration of such devices into large power systems, a balance between power electronics model fidelity and system-level computational efficiency is critical. In system-level simulations of bulk power systems dominated by synchronous generators, detailed electromagnetic models of back-to-back converters may be unnecessary and also computationally inefficient. This paper focuses on developing a simple phasor model for back-to-back converters that can be easily integrated into powerflow solvers to facilitate large-scale power system simulations. The model is implemented using C++ language and integrated into GridLAB-D, an open source software for distribution systems studies, as a potential new capability. The GridLAB-D phasor domain model is validated against the electromagnetic transient (EMT) simulation of the detailed switching model. Simulation results show that the phasor model successfully captures the dominant dynamics of the converter with significantly shorter simulation elapsed time.

Index Terms—Back-to-Back Converter, Phasor Model, Microgrid Building Blocks (MBB), GridLAB-D

I. INTRODUCTION

Power systems are evolving rapidly with increasing deployment of power electronics interfaced energy resources, microgrids, and hybrid AC/DC system. Among these technologies, the microgrid concept appears to be as one of the promising solutions for the operational and planning challenges facing this grid transformation. To enable fast and reliable deployment of microgrids a concept called microgrid building block (MBB) has been proposed [1]. MBB is an idea that provides a high-level concept for standardizing and combining power electronic interfaces, communication and control blocks to form and operate microgrids.

The U.S. Department of Energy (DOE) has invested in developing the MBB-based microgrid concept further to standardize the various blocks needed to enable fast deployment of microgrids to provide energy security and energy resilience. A key MBB block is the power converter interface block that has a back-to-back (BTB) converter at the point of common coupling for a microgrid.

The last couple of decades have seen active development of the BTB converter technology that is effectively applied to various microgrid applications. Some of the key features offered by BTB converters include disturbance isolation, grid

support, bulk grid interconnection and bidirectional power control and conditioning, etc. [2]–[4]. The key applications that overlap with MBB applications [1] are:

- 1) Fault isolation;
- 2) Power conditioning and power flow control;
- 3) Smooth islanding and re-synchronizing (anti-islanding) operation;
- 4) DC microgrid integration.

System level simulations for various configurations of microgrids and networked microgrids built based on the MBB concept will need phasor domain models for the various converters. There are well developed and mature models for smart inverters and other power electronic converters [5]–[7]. However, very few of these models have been integrated and incorporated into three-phase unbalanced power system simulators, as in [8]–[10].

Existing literature has presented detailed EMT simulations for applications of BTB converters in improving the power grid operations [2], [3], [11]–[13]. However, for scalable system-level analysis, it is important to develop models for the BTB converter that can be used in electromechanical time scale simulations, i.e. phasor domain dynamic models.

This paper describes the details of a phasor domain dynamic model for a BTB converter that can be integrated into T&D phasor co-simulation platforms [14] where a DC-link could be used to isolate two networks. The C++ source code of the phasor model is integrated into GridLAB-D software to validate the model, and to add it as a new capability for this software. GridLAB-D [15] is an open source distribution system solver with several power electronics converters' dynamic models in the phasor domain, and can be used for distribution system, microgrid, and T&D co-simulations [14], [16], [17]. However, GridLAB-D currently does not have the capability of simulating a BTB converter. An updated version of GridLAB-D with this capability, based on this work, will be publicly available in the near future.

The BTB converter model is implemented using three objects representing the two converters and the DC-link to enable its integration into two separate networks isolated by a DC-link. The steps involved in integrating such a model with power system solvers are explained along with the interaction between the dynamic solution of the model and that of the system-level.

This paper is accepted for publication in IEEE PESGM 2024. The complete copyright version will be available on IEEE Xplore when the conference proceedings are published.

The GridLAB-D phasor domain BTB converter model is validated against the electromagnetic transient (EMT) simulation of the detailed switching model of the BTB converter developed in MATLAB/Simulink.

The rest of the paper is organized as follows. In Section II, the main phasor equations of the BTB converter are introduced. In Section III, the implementation of the phasor model of the BTB converter is discussed. The GridLAB-D simulation results and validation of the implemented model are presented in Section IV, and conclusions and future work are discussed in Section V.

II. PHASOR EQUATIONS OF THE BACK-TO-BACK CONVERTER

Phasor equations of the back-to-back (BTB) converter are introduced in this section to understand the assumptions and simplifications that will be used in Section III. A simplified diagram of a typical BTB converter is shown in Fig.1. Subscripts g and m are used for the grid-side converter (GSC) and the microgrid-side converter (MSC), respectively. Fig.1 shows an axis transformation block on each side of the BTB converter indicating the transformation from the network frame to the converter frame on each side. These frames are illustrated in Fig. 2. Voltages at the points of common coupling (PCC) $V_g\angle\theta_g$ and $V_m\angle\theta_m$ are provided in the network frames by the power flow solvers on each side during the calculation of the transient response. Phasor equations for the converters are presented below.

The GSC is responsible for regulating the DC-link voltage by controlling its output power in the grid following mode. In this case, the reference for output active power is determined by the DC-link voltage controller. Accordingly, the converter dq frame is synchronized with the grid voltage phasor using a phase-locked-loop (PLL), i.e. $V_g = V_{gd}$ and $V_{gq}=0$ as shown in Fig. 2(b), where $V_g\angle\theta_g$ is provided by the power flow algorithm, at each time step.

The grid current component I_{gd} follows the reference current I_{gd}^* determined by the DC-link controller, while I_{gq} tracks the reference I_{gq}^* which is determined by the voltage controller or the reactive power controller. The variable that plays a major role in integrating the converter into power system solver is the internal voltage (filter Capacitor voltage), which is calculated from Fig. 1 using Kirchhoff's Voltage Law (KVL) as:

$$E_{source-gd} = V_{gd} + R_g I_{gd} - \omega_g L_g I_{gq}, \quad (1a)$$

$$E_{source-gq} = V_{gq} + R_g I_{gq} + \omega_g L_g I_{gd} \quad (1b)$$

Similarly the d - and q -axis current components of the GSC filter current I_{fg} are calculated as:

$$I_{fg-d} = I_{gd} - \omega_g C_{fg} E_{source-gq}, \quad (2a)$$

$$I_{fg-q} = I_{gq} + \omega_g C_{fg} E_{source-gd}, \quad (2b)$$

where ω_g is the radial frequency of the grid. Similarly, the d - and q -axis voltages at the switching terminals of GSC (V_{tg-d} and V_{tg-q}) are calculated using the KVL as:

$$V_{tg-d} = E_{source-gd} + R_{fg} I_{fg-d} - \omega_g L_{fg} I_{fg-q}, \quad (3a)$$

$$V_{tg-q} = E_{source-gq} + R_{fg} I_{fg-q} + \omega_g L_{fg} I_{fg-d}. \quad (3b)$$

Using V_{tg} and I_{fg} , and assuming negligible losses in the converter, the power supplied by the DC-link capacitor into the GSC (P_{dc-g}) and the associated current I_{dc-g} are calculated as:

$$P_{dc-g} = \frac{3}{2}(V_{tg-d}I_{fg-d} + V_{tg-q}I_{fg-q}), \quad (4a)$$

$$I_{dc-g} = \frac{P_{dc-g}}{V_{dc}}, \quad (4b)$$

where V_{dc} is the DC-link voltage. Equations (1)-(4) are used also for the MSC by replacing the subscript g with m . Accordingly, V_{dc} can be calculated using currents exchanged by the converters with the DC-link as:

$$V_{dc} = \frac{1}{C_{dc}} \int (-I_{dc-g} - I_{dc-m}) dt, \quad (5)$$

where I_{dc-m} is the DC-link current supplied by the capacitor into the MSC.

Since the GSC is responsible for regulating the DC link voltage V_{dc} , the grid current component I_{gd} is controlled to follow the reference current I_{gd}^* determined by the active power reference P_g^* generated by the DC-link voltage controller. On the other hand, I_{gq} is determined by the reactive power reference Q_g^* . Hence, the reference currents are generated by

$$I_{gd}^* = \frac{2}{3} \frac{P_g^*}{V_{gd}}, \quad (6a)$$

$$I_{gq}^* = \frac{-2}{3} \frac{Q_g^*}{V_{gd}}, \quad (6b)$$

where,

$$P_g^* = K_P(V_{dc} - V_{dc}^*) + K_I \int (V_{dc} - V_{dc}^*) dt. \quad (6c)$$

The reference Q_g^* is either received as a dispatch command or generated using a local grid voltage controller. In phasor domain simulation of bulk power systems, since the electromechanical dynamics dominate the transient response, the current controller dynamics are approximated by a first-order low pass filter of a certain time constant T_f .

$$T_f \frac{dI_{gd}}{dt} + I_{gd} = I_{gd}^*, \quad (7a)$$

$$T_f \frac{dI_{gq}}{dt} + I_{gq} = I_{gq}^*. \quad (7b)$$

III. SIMPLIFIED PHASOR MODEL IMPLEMENTATION

The BTB converter phasor model source code is written in C++ and integrated into GridLAB-D software as a new simulation capability. To achieve this integration, the converter on each side of the DC-link is first represented as a voltage source behind an impedance, as shown in Fig. 3(a), for the grid side [5], [9]. The voltage behind the impedance is E_{source} which is the voltage at the filter capacitor, whereas the impedance represent the interface reactor and its resistance. Thereafter, the Norton equivalent circuit is used, as shown in Fig. 3(b), to integrate it into the power flow solver of GridLAB-D software.

Because of the unique nature of the BTB converter, where the grid and microgrid networks are isolated and solved

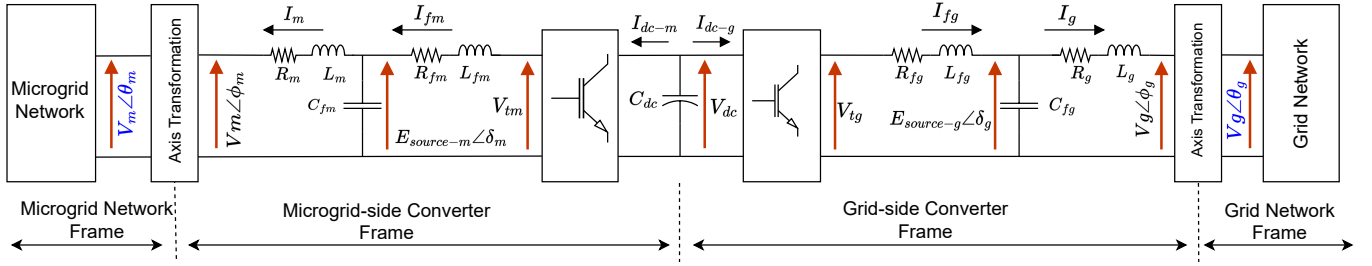


Fig. 1. Back-to-back converter connected to a grid and a microgrid network.

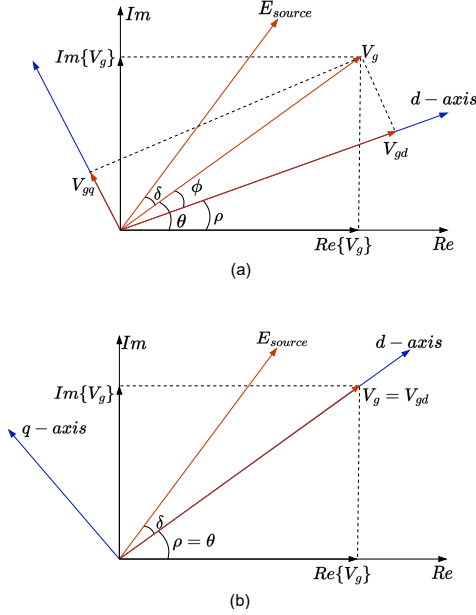


Fig. 2. Network and converter frames, where the dq frame represents the converter side, while the Re/Im frame represent the network side. (a) A general case; (b) the case when the dq frame is aligned with the network terminal voltage using a PLL, i.e. $V_g = V_{gd}$ and $V_q = 0$.

separately, the BTB converter is implemented in GridLAB-D using three objects. These objects are the GSC object with the DC-link controller, the MSC object, and the DC-link object, which can exchange data with each other and the network solvers as shown in Fig. 4. The focus here will be on the dynamic simulation of the GSC since it is the one considered in charge of the DC-link regulation. Dynamic simulation of the MSC follows similar steps, with more additional flexibility in operating it as a grid forming or a grid following converter.

The steps to compute the transient response of the GSC and the DC-link are briefly discussed in the following:

- 1) If a disturbance occurs in the network at time t , such as a load change or a fault, the network admittance matrix is updated and loads are calculated as fixed impedances.
- 2) In the network solver, using the initial $E_{source-g}$ or $I_{g-source-g}$ and other generators internal voltages, the bus voltage V_g is calculated at time t . Similar calculations are performed for all the generators in the network.
- 3) The GSC receives the updated V_g and uses the initial $I_{source-g}$ and Norton equivalent to calculate the initial value for I_g in the network frame.

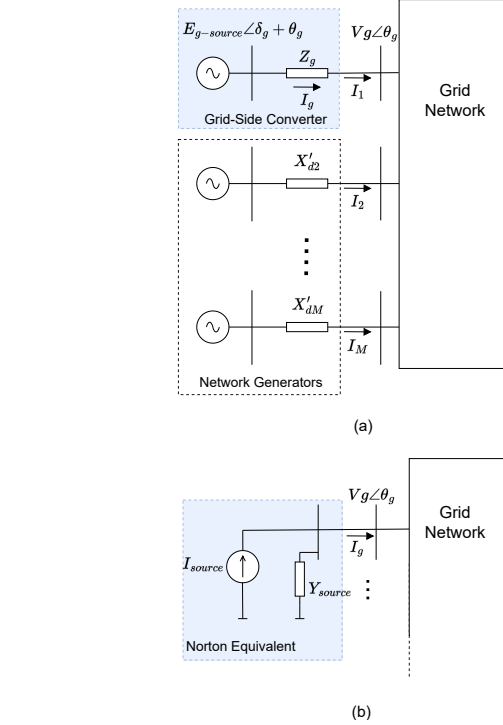


Fig. 3. Thevenin and Norton representation of the GSC and the grid networks. (a) Thevenin equivalent; (b) Norton equivalent

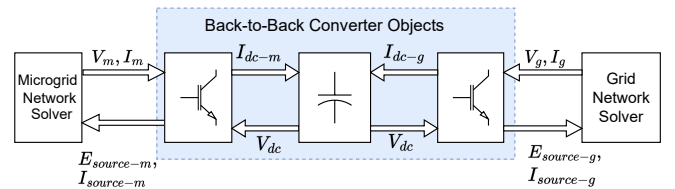


Fig. 4. Three-object structure implementation and data exchange of the back-to-back converter in GridLAB-D.

- 4) The GSC converts I_g and V_g into the converter frame using the axis transformation in Fig. 2(b).
- 5) The GSC uses the transformed values to update $E_{source-g}$ at t using equation (1).
- 6) Ignoring the filter losses, and using the V_{dc} value from the DC-Link object, the power and current at the DC-link

TABLE I
BACK-TO-BACK CONVERTER PARAMETERS

Parameter	Value
Ph-Ph rms grid voltage, V_g	208 V
Ph-Ph rms microgrid voltage, V_m	208 V
Grid-Side Converter kVA, S_{GSC}	50 kVA
Microgrid-Side Converter kVA, S_{MGSC}	50 kVA
R_g	0.001 Ω
L_g	0.2 mH
C_{fg}	50 μ F
R_{fg}	0.001 Ω
L_{fg}	1 mH
R_m	0.001 Ω
L_m	0.2 mH
C_{fm}	50 μ F
R_{fm}	0.001 Ω
L_{fm}	1 mH
C_{dc}	5000 μ F
V_{dc}^*	600 V
Switching frequency (for the detailed model)	20 kHz

TABLE II
BACK-TO-BACK CONVERTER CONTROL PARAMETERS

Parameter	Value
DC-link voltage regulator K_P	700 W/V
DC-link voltage regulator K_I	800 W/(V.s)
Current loop time constant T_f	0.005 s

can be calculated at time t as:

$$P_{dc-g} = \frac{3}{2}(E_{source-gd}I_{gd} + E_{source-gq}I_{gq}), \quad (8a)$$

$$I_{dc-g} = \frac{P_{dc-g}}{V_{dc}}. \quad (8b)$$

- 7) **Predictor Iteration:** Execute the first step of Euler's modified method
 - a) Compute the preliminary estimates of the grid current references, \tilde{I}_{gd}^* and \tilde{I}_{gq}^* , at $(t + \Delta t)$ using equation (6).
 - b) Compute the preliminary estimates of the grid currents, \tilde{I}_{gd} and \tilde{I}_{gq} , using equation (7) with \tilde{I}_{gd}^* and \tilde{I}_{gq}^* as their inputs, respectively.
 - c) Calculate $\tilde{E}_{source-g}$ and $\tilde{I}_{source-g}$, convert them to the network frame, and provide them to the network solver.
- 8) The network solver calculate a preliminary estimate of the bus voltage \tilde{V}_g at time $t + \Delta t$
- 9) Repeat steps (2-6).
- 10) **Corrector Iteration:** Execute the second step of Euler's modified method to compute the final values of I_{gd} , I_{gq} , and I_{dc-g} at $t + \Delta t$.
- 11) Share I_{dc-g} with the DC-Link object.
- 12) Calculate the final bus voltage V_g at time $t + \Delta t$.
- 13) Set $(t = t + \Delta t)$; the DC-link object calculates the DC-link voltage using equation (5), and I_{dc-m} and I_{dc-g} values.
- 14) Stop if $t > T_{stop}$; otherwise, go to Step 1.

TABLE III
SIMULATION TIME

Simulation Type	Simulation Time	Elapsed Real Time
EMT	20 s	1020 s
Phasor	20 s	9 s

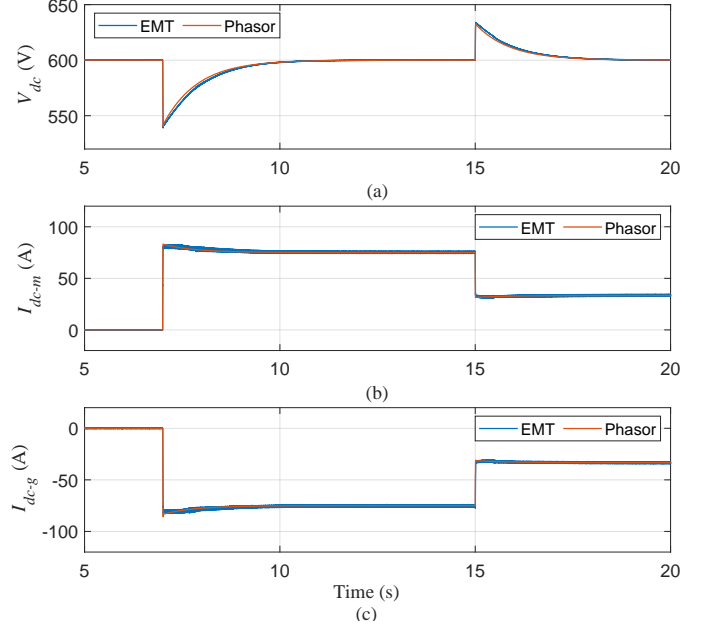


Fig. 5. Model performance in response to variations in the power imported by the microgrid. (a) DC-link voltage, (b) DC-link current flowing into the MSC (I_{dc-m}), and (c) DC-link current flowing into the GSC (I_{dc-g}).

IV. VALIDATION OF PHASOR DOMAIN DYNAMIC MODEL

This section shows the simulation results of the phasor domain model, of the system shown in Fig.1, implemented in GridLAB-D using the developed objects. The system is also implemented in MATLAB/Simulink to perform EMT simulations. The system and corresponding control parameters are ensured to be the same in both models. The GSC and MSC are connected to ideal voltage sources.

The simulation time steps in GridLAB-D simulations are maintained at 1ms. The detailed switching model of the BTB converter is simulated at a 1μ s solver time step, and both models are simulated on a computer equipped with Intel(R) Core i7-1185G7 running at 3 GHz, and 16 GB of memory.

The power set-points of MSC are varied to demonstrate the dynamics of the DC-link and the GSC and MSC controllers. As the BTB model is intended to interface the microgrid at the point of common coupling, two operating scenarios are used for validating the model. The first case is when the microgrid imports power from the grid (grid-side); and, the second case is when the microgrid recers power flow to export power to the grid-side. Table I shows the grid, microgrid, and BTB converter parameters and Table II shows the key control parameters of the BTB converter.

The the elapsed real time for the EMT simulation is significantly greater than that required for the phasor simulation as shown in Table III.

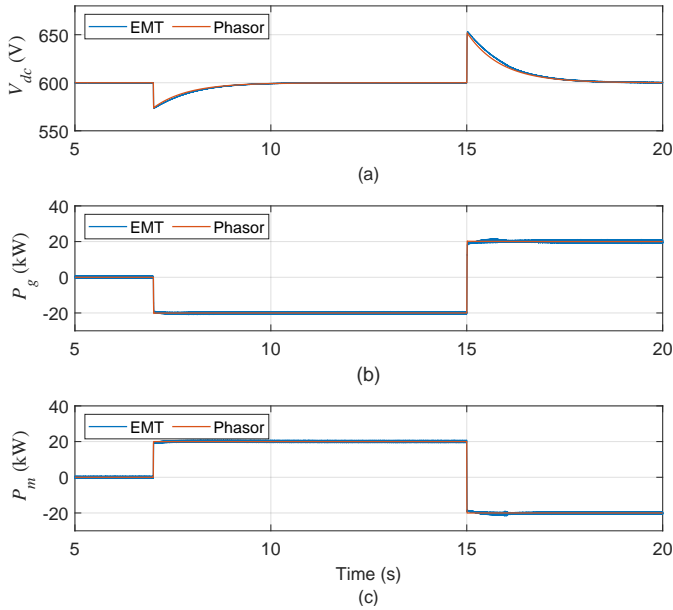


Fig. 6. Model performance in response to power variations and power flow reversal. (a) DC-link voltage, (b) Grid side converter power (P_g), and (c) Microgrid side converter power (P_m).

A. Power Flow from Grid to Microgrid

This operating scenario is a usual operating scenario for a grid-connected microgrid. To focus on the DC-link object performance, Fig. 5 shows the DC-link voltage and currents behaviors in response to the changes in the microgrid imported power. In this scenario, the MSC power set point is changed from 0 to 45 kW at $t=7$ s, and then dropped to 20 kW at $t=15$ s. To show the dc currents dynamic behavior, the currents in the EMT simulation are filtered with first order filter with a time constant of 1 ms. The results show the transient and the steady-state response of the DC voltage and currents closely match between GridLAB-D and MATLAB/Simulink EMT simulations. Results also indicate that the proposed three-object implementation of the BTB and the data exchange among objects are integrated successfully into the power flow solver of GridLAB-D software.

B. Bi-Directional Power Flow Between Grid and Microgrid

In this scenario the bi-directional power flow, between grid and microgrid, is examined. Figs. 6 show the DC-link voltage and power output at the grid-side and microgrid-side during a power flow direction reversal. In this scenario, the MSC power set point (P_m^*) is changed from 0 to 20 kW at time $t=7$ s, and then from 20 kW to -20 kW at $t=15$ s.

The responses of the phasor domain model and the EMT model to these set point changes are shown in Fig. 6(b) for the grid-side and in Fig. 6(c) for the microgrid-side. The DC-link voltage and power flow between grid and microgrid closely match for both simulation models.

V. CONCLUSIONS

To enable large scale system simulation that focus on electromechanical dynamics, a phasor domain model of BTB

converter is developed and validated in this paper. The model is implemented in GridLAB-D software to demonstrate its applicability for system-level dynamic simulations. Preliminary simulations and analysis show that the phasor model captures the dominating dynamics of the detailed switching model. Simulation results show that the proposed three-object implementation of the BTB and the data exchange among objects are integrated successfully into the power flow solver of GridLAB-D software. The developed phasor domain model enables easy implementation of BTB converters and can be integrated into other power system software directly or through user defined models. This work will be extended to perform various system-level simulations for different use cases showcasing benefits of interfacing a microgrid using a BTB converter in grid-connected and networked microgrids.

ACKNOWLEDGMENT

The authors wish to thank Dan Ton with the U.S. Department of Energy, Office of Electricity for funding this work.

REFERENCES

- [1] Building Blocks for Microgrids. Accessed: June 8, 2023. [Online]. Available: <https://www.energy.gov/sites/default/files/2022-09/3-Building%20Blocks%20for%20Microgrids.pdf>
- [2] R. Majumder, A. Ghosh, G. Ledwich, and F. Zare, "Power management and power flow control with back-to-back converters in a utility connected microgrid," *IEEE Transactions on Power Systems*, vol. 25, no. 2, pp. 821–834, 2010.
- [3] R. Majumder, "A hybrid microgrid with dc connection at back to back converters," *IEEE Transactions on Smart Grid*, vol. 5, no. 1, pp. 251–259, 2014.
- [4] C.-Y. Tang, Y.-F. Chen, Y.-M. Chen, and Y.-R. Chang, "Dc-link voltage control strategy for three-phase back-to-back active power conditioners," *IEEE Transactions on Industrial Electronics*, vol. 62, no. 10, pp. 6306–6316, 2015.
- [5] W. Du, Y. Liu, R. Huang, F. K. Tuffner, J. Xie, and Z. Huang, "Positive-sequence phasor modeling of droop-controlled, grid-forming inverters with fault current limiting function," in *2022 IEEE Power & Energy Society Innovative Smart Grid Technologies Conference (ISGT)*, 2022, pp. 1–5.
- [6] C. T. Rim, *Phasor Power Electronics*. Springer, 2016.
- [7] P. Santiprapan, K.-L. Areerak, and K.-N. Areerak, "Mathematical model and control strategy on dq frame for shunt active power filters," *International Journal of Electrical and Computer Engineering*, vol. 5, no. 12, pp. 1669 – 1677, 2011. [Online]. Available: <https://publications.waset.org/vol/60>
- [8] Y. Li, Y. Gu, and T. C. Green, "Revisiting grid-forming and grid-following inverters: A duality theory," *IEEE Transactions on Power Systems*, vol. 37, no. 6, pp. 4541–4554, 2022.
- [9] W. Du, F. K. Tuffner, K. P. Schneider, R. H. Lasseter, J. Xie, Z. Chen, and B. Bhattarai, "Modeling of grid-forming and grid-following inverters for dynamic simulation of large-scale distribution systems," *IEEE Transactions on Power Delivery*, vol. 36, no. 4, pp. 2035–2045, 2021.
- [10] A. Quedan, W. Wang, D. Ramasubramanian, E. Farantatos, and S. Asgarpour, "Dynamic behavior of combined 100% ibr transmission and distribution networks with grid-forming and grid-following inverters," in *2023 IEEE Power & Energy Society Innovative Smart Grid Technologies Conference (ISGT)*, 2023, pp. 1–5.
- [11] Y.-T. Chen, Y.-F. Chen, C.-Y. Tang, Y.-M. Chen, and Y.-R. Chang, "An active power conditioner with a multi-mode power control strategy for a microgrid," in *2013 1st International Future Energy Electronics Conference (IFEEEC)*, 2013, pp. 93–97.
- [12] H. Akagi and R. Kitada, "Control and design of a modular multilevel cascade btb system using bidirectional isolated dc/dc converters," *IEEE Transactions on Power Electronics*, vol. 26, no. 9, pp. 2457–2464, 2011.
- [13] C. Liu, B. Wu, N. R. Zargari, D. Xu, and J. Wang, "A novel three-phase three-leg ac/ac converter using nine igbts," *IEEE Transactions on Power Electronics*, vol. 24, no. 5, pp. 1151–1160, 2009.

- [14] A. K. Bharati and V. Ajjarapu, "SMTD co-simulation framework with helics for future-grid analysis and synthetic measurement-data generation," *IEEE Transactions on Industry Applications*, vol. 58, no. 1, pp. 131–141, 2022.
- [15] D. P. Chassin, K. Schneider, and C. Gerkenmeyer, "GridLAB-D: An open-source power systems modeling and simulation environment," in *2008 IEEE/PES Transmission and Distribution Conference and Exposition*. IEEE, 2008, pp. 1–5.
- [16] A. K. Bharati and V. Ajjarapu, "A scalable multi-timescale t&d co-simulation framework using helics," in *2021 IEEE Texas Power and Energy Conference (TPEC)*, 2021, pp. 1–6.
- [17] A. K. Bharati, V. Ajjarapu, W. Du, and Y. Liu, "Role of distributed inverter-based-resources in bulk grid primary frequency response through helics based SMTD co-simulation," *IEEE Systems Journal*, vol. 17, no. 1, pp. 1071–1082, 2023.